



Western Washington University  
Western CEDAR

---

WWU Graduate School Collection

WWU Graduate and Undergraduate Scholarship

---


2013

## Voltage-sensitive gating of the Pannexin-1 channel

Margaret A. Fuqua

*Western Washington University*

Follow this and additional works at: <https://cedar.wwu.edu/wwuet>

 Part of the [Biology Commons](#)

---

### Recommended Citation

Fuqua, Margaret A., "Voltage-sensitive gating of the Pannexin-1 channel" (2013). *WWU Graduate School Collection*. 393.

<https://cedar.wwu.edu/wwuet/393>

This Masters Thesis is brought to you for free and open access by the WWU Graduate and Undergraduate Scholarship at Western CEDAR. It has been accepted for inclusion in WWU Graduate School Collection by an authorized administrator of Western CEDAR. For more information, please contact [westerncedar@wwu.edu](mailto:westerncedar@wwu.edu).

**Voltage-Sensitive Gating of the Pannexin-1 Channel**

By  
Margaret A. Fuqua

Accepted in Partial Completion  
Of the Requirements for the Degree  
Master of Science

Kathleen L. Kitto, Dean of the Graduate School

ADVISORY COMMITTEE

Chair, Dr. José R. Serrano-Moreno

Dr. Joann J. Otto

Dr. Jacqueline K. Rose

## **MASTER'S THESIS**

In presenting this thesis in partial fulfillment of the requirements for a master's degree at Western Washington University, I grant to Western Washington University the non-exclusive royalty-free right to archive, reproduce, distribute, and display the thesis in any and all forms, including electronic format, via any digital library mechanisms maintained by WWU.

I represent and warrant this is my original work, and does not infringe or violate any rights of others. I warrant that I have obtained written permissions from the owner of any third party copyrighted material included in these files.

I acknowledge that I retain ownership rights to the copyright of this work, including but not limited to the right to use all or part of this work in future works, such as articles or books.

Library users are granted permission for individual, research and non-commercial reproduction of this work for educational purposes only. Any further digital posting of this document requires specific permission from the author.

Any copying or publication of this thesis for commercial purposes, or for financial gain, is not allowed without my written permission.

Margaret Fuqua  
May 10, 2013

# **Voltage-Sensitive Gating of the Pannexin-1 Channel**

A Thesis  
Presented to  
the Faculty of  
Western Washington University

In Partial Fulfillment  
of the Requirements for the Degree  
Master of Science

By  
Margaret A. Fuqua  
May 2013

## Voltage-Sensitive Gating of the Pannexin-1 Channel

By, Margaret A. Fuqua

### ABSTRACT

Since its discovery just over a decade ago, Pannexin-1 (Px1) has been recognized in a number of important physiological and pathophysiological processes such as taste, inflammation, and tumor suppression. This large-pore, polymodal ion channel was initially identified as ‘voltage-dependent,’ though there have been no precise studies concerning the gating properties of Px1 to date. Because Px1 is expressed in excitable cells, identifying voltage-gating properties of Px1 was our primary goal. Using the two-electrode voltage clamp technique, we showed for the first time that Px1 is a weakly voltage-gated channel. Depolarizing voltages up to +200 mV revealed half-maximal activation at +51 mV and a weak voltage-dependence through generation of a complete Boltzmann activation curve. We also showed that Px1 activates in < 3.5 ms, consistent with the time frame of action potentials (1-4 ms). Opening rates of Px1 also seemed to be very weakly voltage-dependent. Further, we showed that Px1 displays consistent current decay at depolarizing voltages greater than +100 mV. Additionally, using two cell systems to exogenously express Px1, we observed a marked decrease of functional Px1 expression within ~24 hours of injection. Taken together, our findings suggest that Px1 is a fast opening, voltage-sensitive channel that may have a number of mechanisms in place to prevent uncontrolled conductivity.

## ACKNOWLEDGMENTS

I would like to sincerely thank everyone who has helped support me through this research process. This includes my friends and family for encouraging me, Dr. Jackie Rose and Dr. Joann Otto for their continual feedback and advice, Dr. David Leaf for honorary committee support and added microscopy training, Dr. Heather VanEpps for encouraging me to pursue graduate education and for her mentorship, and Peter Thut, Jeannie Gilbert, Mark Price, and Kendra Bradford for their unending assistance with teaching, technical, and moral support. I would additionally like to thank Dr. Joann Otto for being a constant source of support in all areas of my academic endeavors, and for helping me in many ways to trust in my potential as a scientist and teacher. For their indispensable assistance with data collection and care of cells, I thank my labmates Matt Hill and Taylor Bunch; they worked tirelessly to help me in aspects of this project I would not have been able to accomplish alone.

We are very thankful to Dr. Gerhard Dahl for donating the mPx1 construct we used for *in vitro* transcriptions for mRNA injection into oocytes. Also, we'd like to thank Dr. Eliana Scemes for donating mPx1-eGFP plasmid for transfection of Neuro2a cells. We are extremely grateful to Dr. William Zagotta and his lab for graciously supplying us with *Xenopus laevis* oocytes for the past 5 years.

I would also like to acknowledge the assistance I've received from CST for financial support, and the WWU Biology Faculty Fellowship and Research and Sponsored Programs grant to help me purchase materials needed to conduct my research.

Finally, I wholeheartedly thank my six-year advisor, mentor, and friend, Dr. José Serrano-Moreno, who has inspired me over these years to be a better scientist, teacher, and individual. He has been my sole educator in membrane physiology and has believed in me from day one—his confidence in me is in large part why I have persisted in the sciences, and I couldn't be more thankful.

## TABLE OF CONTENTS

ABSTRACT.....	IV
ACKNOWLEDGMENTS .....	V
LIST OF FIGURES.....	VII
LIST OF TABLES .....	VIII
LIST OF ABBREVIATIONS .....	IX
1. INTRODUCTION .....	1
1.1 ION CHANNELS .....	3
1.2 GATING OF ION CHANNELS.....	5
1.3 VOLTAGE-SENSITIVITY OF <i>Px1</i> .....	7
2. METHODS .....	9
2.1 IN VITRO TRANSCRIPTION .....	9
2.2 MICROINJECTION OF OOCYTES .....	9
2.3 SOLUTIONS.....	10
2.4 TWO-ELECTRODE VOLTAGE CLAMP (TEVC).....	10
2.5 DATA ANALYSIS .....	11
3. RESULTS .....	12
3.1 ISOLATION OF <i>Px1</i> CURRENT.....	12
3.2 VOLTAGE-DEPENDENCE OF <i>Px1</i> CURRENTS .....	12
3.3 ACTIVATION KINETICS OF <i>Px1</i> .....	15
3.4 LARGE OOCYTE-SPECIFIC CURRENT ELICITED AT HIGH VOLTAGES.....	18
3.5 CURRENT DECAY OF <i>Px1</i> .....	21
4. DISCUSSION.....	24
4.1 <i>Px1</i> IS A VOLTAGE-SENSITIVE CHANNEL .....	24
4.2 ACTIVATION OF <i>Px1</i> .....	27
4.3 CURRENT DECAY OF <i>Px1</i> .....	33
4.4 <i>Px1</i> TURNOVER RATE SUGGESTS POSSIBLE REGULATION MECHANISM.....	35
4.5 CONCLUSION .....	37
5. BIBLIOGRAPHY.....	39

## LIST OF FIGURES

<b>Figure 1.</b> General ion channel anatomy.....	5
<b>Figure 2.</b> Simple kinetics scheme depicting open, closed, and inactivated states.....	6
<b>Figure 3.</b> Pharmacological isolation of Px1 current.....	13
<b>Figure 4.</b> Current-voltage (I-V) relationship of Px1 with +60 mV protocol.....	14
<b>Figure 5.</b> Activation curve of Px1 with +60 mV protocol.....	16
<b>Figure 6.</b> Px1 current and activation curve with +200 mV protocol.....	17
<b>Figure 7.</b> Activation rates of Px1 at +150 mV, 100 mV, and 50 mV.....	19
<b>Figure 8.</b> Oocytes exhibit increased outward current at high voltages.....	20
<b>Figure 9.</b> Isolated Px1 current showed slow current decay.....	23
<b>Figure 10.</b> Proposed arrangement of Px1 monomer.....	32



## LIST OF TABLES

<b>Table 1.</b> Boltzmann parameters of select voltage-dependent channels.....	25
--	----

## LIST OF ABBREVIATIONS

ATP	Adenosine 5'-triphosphate
CBX	carbenoxolone
CD	current decay
Cx	Connexin
Il-1 $\beta$	Interleukin-1 $\beta$
Inx	Innexin
mRNA	messenger RNA
NMDA	<i>N</i> -methyl-D-aspartate
Px1	Pannexin-1
SCAM	substituted cysteine accessibility method
VSD	voltage sensing domain

## 1. INTRODUCTION

Pannexin-1 (Px1) has been suggested to play multiple roles in biologically important processes such as tumor suppression, taste bud reception, activation of the inflammasome, and seizure-like activity in the hippocampus (Lai et al., 2007; Penuela et al., 2012; Silverman et al., 2009; Pelegrin and Surprenant, 2006; Sandilos et al., 2012; Huang et al., 2007). Along with Connexins (Cx) and Innexins (Inx), Pannexin-1 (Px1) is a member of the gap junction protein family, which is characterized by pores large enough to pass polyatomic ions such as neurotransmitters and ATP (Iglesias et al., 2009; Bao et al., 2004; Locovei et al., 2006a). Topologically similar to Cx, Px1 has an anticipated membrane topology including four transmembrane segments, two extracellular loops, and intracellular N- and C-termini (Wang and Dahl, 2010). Unlike connexins, however, Px1 does not participate in canonical gap junction plaque formation. This is likely due to the fact that Px1 is glycosylated at positions along its extracellular loops and is physically incapable of docking with opposing channels (Boassa et al., 2007; MacVicar and Thompson, 2010; Penuela et al., 2007). This feature of Px1 thus allows exchange of ions or small molecules to occur between the intracellular and extracellular space.

Px1 has been documented as a 'voltage-dependent' channel, and is ubiquitously expressed in both vertebrates and invertebrates (Billaud et al., 2012). Px1 can be opened in response to a multitude of factors including caspase cleavage of the intracellular C-terminus (Sandilos et al., 2012), mechanical stress (Bao et al., 2004), increased intracellular  $\text{Ca}^{2+}$  (Locovei et al., 2006c), as well as depolarization of the cell membrane (Thompson et al., 2008a). The proposed large pore size of Px1 and its suggested ability to pass ATP, cytokines, and other large polyatomic ions in numerous cell types make Px1 a protein of particular

interest to addressing questions regarding purinergic cell signaling and the innate immune response (Qiu and Dahl, 2009; Sandilos et al., 2012; Li and Banerjee, 2011). Further, the suggested voltage-dependent properties and presence of Px1 in excitable cell types such as neurons and cardiomyocytes make the voltage-gating characteristics of Px1 a topic of importance for signaling in the cardiovascular and central nervous systems.

Until recently, the most widely studied of the gap junction proteins were the connexins (Cx). Cx hemichannels (or half gap junction channel) demonstrate strong inhibition (stabilizing occupancy of the closed state) by divalent cations such as calcium and magnesium, as well as complex voltage-dependent gating. These qualities render Cx hemichannels to be open only in situations of severe ionic dysregulation, but not in standard physiological conditions (Thompson and MacVicar, 2008). Pannexin, seems to be a more likely candidate for opening in physiological conditions (Bruzzone et al., 2003). Since pannexins have not been found to form gap junctions and display no inhibition by extracellular cations (MacVicar and Thompson, 2010), it is suggested that the functional unit of pannexin is an unopposed hemichannel (Locovei et al., 2006b). In this regard, it should be noted that Px1 has since been referred to as simply a ‘channel;’ since Px1 does not form gap junctions, the ‘hemi’ form does not technically exist for Px1. Consistent with this view, it has been suggested that Px1 channels can permit fluxes of molecules such as ATP and glutamate (Sandilos et al., 2012; Orellana et al., 2011). These molecules are associated with cellular tasks involving immune response (Silverman et al., 2009), taste sensation (Huang et al., 2007), neural/glia transmission (MacVicar and Thompson, 2010), and paracrine and autocrine signaling (Locovei et al., 2006b). For example, Px1 has been suggested to be involved in bursting events at postsynaptic sites in the hippocampus (Thompson et al.,

2008a), as well as involvement in taste bud receptor activation and ATP signaling (Chaudhari and Roper, 2010). Because opening the P<sub>x</sub>1 channel appears to be voltage-dependent under physiological concentrations of divalent cations, unlike C<sub>x</sub> hemichannels, this suggests significant activity of P<sub>x</sub>1 channels in excitable cells like those in the nervous system.

Additionally, P<sub>x</sub>1 has been implicated in activation of the inflammation response by triggering a multiprotein complex called the inflammasome in macrophages (Silverman et al., 2009). Such activation involves assembly of a complex that ultimately activates caspases required for inflammatory response and interleukin-1 $\beta$  (Martinon et al., 2002; Silverman et al., 2009; Martinon et al., 2009). Studies suggest that P<sub>x</sub>1 is involved in formation of the inflammasome by interacting with the purinergic receptor P2X<sub>7</sub>, which can be activated by extracellular ATP. P<sub>x</sub>1 subsequently seems to activate caspase-1, which mediates the transition between pro-interleukin1 $\beta$  (pro-IL-1 $\beta$ ) to active IL-1 $\beta$  (Silverman et al., 2009). It seems that inflammatory responses are additionally present in neurons and astrocytes (Bennett et al., 2012) and as a proposed voltage-dependent channel, it seems that voltage-gating of the P<sub>x</sub>1 channel is necessary to understand modes of regulating potential inflammatory responses in the brain. To better conceptualize the purpose of our study, we will briefly review the fundamentals of ion channels and introduce the concept of voltage-dependent gating.

### 1.1 *Ion channels*

The structural integrity of a cell membrane is essential for all life. Cell membranes have exquisite selective permeability, and only allow small molecules such as oxygen and carbon dioxide to diffuse into and out of the cell. To bring in nutrients or expel wastes, cells must also have tightly regulated ion channels and transporters to control these fluxes.

Channels are a necessary component for cells to control osmotic stress, a primary threat to a selectively permeable membrane. Should a cell experience an influx of ions, cells can respond by expelling other ions through channels to reduce osmotic pressure (Reyes et al., 2010). Channels can also be a conduit for signaling ions such as calcium, triggering important cellular processes in response to changing intracellular and extracellular environments (Huang et al., 2007; Silverman et al., 2009; Woehrle et al., 2010).

Deciphering the specific functions and regulation mechanisms of ion channels is essential to understanding their numerous important roles in cell physiology. The ability of a cell to survive the constantly fluctuating conditions of living organisms requires very tight control of ion channels and transporters; maintaining ionic concentration gradients, facilitating exchange of nutrients and waste products, and actively communicating with other cells via molecular signaling pathways are all made possible by these crucial membrane proteins.

Typically, ion channels are conduits for single ions to pass through a cell membrane to control ionic gradients for a number of purposes. Px1 is a unique channel, as it seems to pass not only ions, but also large polyatomic ions and small molecules. The significance of Px1 as a channel is that when it is open, select ions or molecules can pass through the channel at the rate of electrodiffusion ( $1 \times 10^6$  ions/sec) down their respective concentration gradients. This implies potential for significant efflux of ATP or other signaling molecules at rates much faster than exocytosis or transporter-mediated fluxes (Thompson and MacVicar, 2008). As previously mentioned, channel-mediated fluxes must be tightly regulated to maintain proper cellular homeostasis; considering the extent of Px1 involvement in multiple biological processes, uncovering how this large-pore channel is regulated is necessary.

## 1.2 Gating of ion channels

Ion channels provide a continuous, water-filled conduit for ions and molecules to pass through at the rate of electrodiffusion. Ions pass through the channel via the 'pore', composed of several identical subunit domains facing each other (Figure 1). Channels open and close by means of 'gating,' a series of conformational changes that result in either 'pore dilation' or opening or closing of a 'gate,' thus permitting or limiting ion flow.

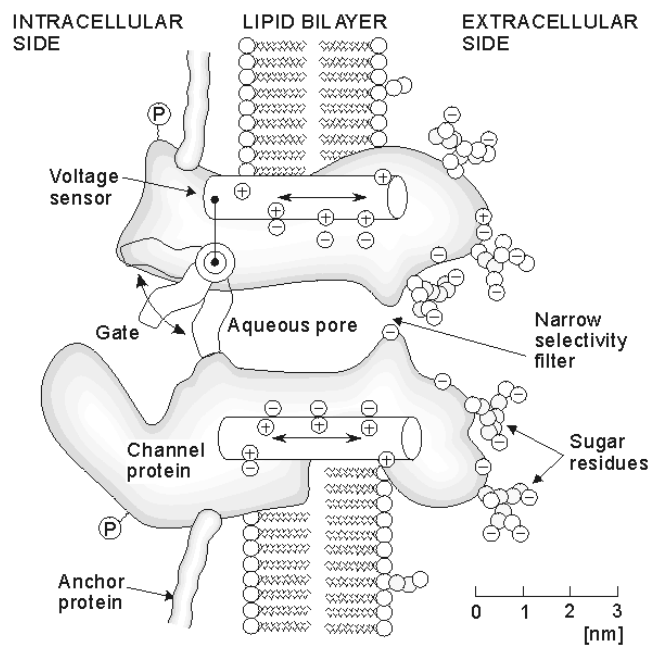


**Figure 1.** General ion channel anatomy (Hille, 1992).

Gating follows the general scheme depicted in figure 2, which includes Closing, Opening, and Inactivation; however, there can be multiple substates to this scheme; for example, some channels can inactivate from the closed state, or have multiple open states.

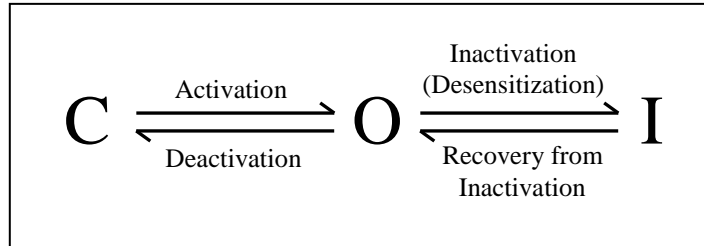


**Figure 2.** Simple kinetics scheme depicting three basic conformational states of ion channels: Closed (C), Open (O), and Inactivated (I). Each arrow indicates the rate of transition between conformational states.

Channel gating can occur by way of many different processes: they can be gated by binding of ligands or small molecules; some are mechanosensitive and respond to processes such as cellular swelling; others are sensitive to changes in pH (ASIC acid sensing channels), and many are also gated by changes in voltage, which is what we focus on in the present study (Yellen, 1998).

These diverse stimuli can alter the rate of occupancy of the channel in each state. One can identify these states by the presence, absence, or decrease of current mediated by the flux of charged particles through the pore in electrophysiological experiments (see equation 1).

$$I = \frac{dQ}{dt} \quad \text{(Equation 1)}$$

In the case of Px1, it is known that positive membrane voltages  $> +20$  mV increase ionic conductance, favoring occupancy of the open state (D'hondt et al., 2009; Bruzzone et al., 2003). There is one account in which prolonged depolarizations of Px1 in *Xenopus laevis*



oocytes seem to promote current decay, which could be evidence of an inactivated state (Bruzzone et al., 2003). Inactivation is defined as a non-conductive state, or ‘absorptive’ state, in which the pore can be open or closed, but non-conductive in either case. Inactivation is a more complicated state, and in some cases can occur simultaneously with the other states if inactivation is dependent on a particular channel conformation.

Because Px1 channels are seemingly voltage-gated and can be open in the presence of divalent cations, it is possible that an action potential is sufficient to open Px1, which could allow significant fluxes of neurotransmitters and/or ATP in a short period of time. Evidence of Px1 activation has been shown as a direct result of NMDA receptor activation in hippocampal neurons (Thompson et al., 2008a). With the relatively recent discovery of Px1, not much is currently known about its gating mechanisms. Because an action potential depolarizes neuronal membranes to ~ +40 mV (higher than the +20 mV required to activate Px1), one question we investigated here is whether the time it takes for an action potential to depolarize a membrane and return to resting voltages (~1-4 ms) is comparable to the activation rates for Px1 (Kandel and Schwartz, 1985). We have shown that Px1 has a fast activation rate comparable to the time-frame of an action potential which could implicate Px1 as a very important component of voltage-regulated cell signaling pathways.

### *1.3 Voltage-sensitivity of Px1*

The Px1 channel is raising new questions in cell physiology because it can not only function as an ion channel, but it can also allow larger molecules to flow across the membrane at rates much faster than transporters. Additionally, Px1 seems to be voltage-gated, and also potentially activated by a number of other voltage-independent mechanisms.

These properties make Px1 largely relevant to excitable cells as well as non-excitable immunological cells.

Considering the physiological importance of the ions and molecules able to pass through Px1 channels, we decided to examine the role of voltage in the opening kinetics of this yet uncharacterized channel. As a proposed ‘voltage-dependent’ channel, it is highly possible that Px1 could be opened by membrane depolarization caused by action potentials or receptor graded potentials. Due to its suggested capability to be opened by N-methyl-D-aspartate (NMDA) receptor activation as well as being a proposed conduit for ATP release, it seems that Px1 could play a role in voltage-mediated purinergic signaling in the central nervous system. Px1 channels are thought to play various roles in taste sensation, seizure and stroke, and activation of the inflammasome (Huang et al., 2007; Thompson et al., 2008a; Silverman et al., 2009), so a better understanding of how Px1 functions can provide information for potential treatment of neurological or immune disorders. It seems plausible that the kinetics of Px1 channels are comparable to that of physiological changes in membrane potentials, so we aimed to better understand the extent to which voltage plays a role in the activation of Px1. Here we exogenously expressed mouse Px1 (mPx1) in *Xenopus laevis* oocytes and utilized standard two electrode voltage clamp techniques to identify gating properties of Px1. The present study is the first report of the relative voltage-sensitivity and activation rate of Px1. We found very little difference in activation rates at different voltages and discovered that Px1 requires large inputs of voltage to achieve maximal activation; together with evidences supporting polymodal gating, these findings have led us to conclude that Px1 is more appropriately termed ‘voltage-sensitive,’ rather than its previous distinction as a voltage-dependent channel.

## 2. METHODS

### 2.1 *In vitro transcription*

Mouse pannexin-1 (mPx1) cDNA was graciously provided by Dr. Gerhard Dahl, University of Miami (Miami, FL). The mPx1 cDNA was inserted into a PCS2 plasmid and linearized using Not1 restriction enzyme (New England Biolabs<sup>®</sup> Inc.). Additional clean-up of linearized cDNA was performed using DNA Clean and Concentrator<sup>™</sup> (Zymo Research Corporation, Irvine, CA). Purified mPx1 cDNA was transcribed into mPx1 mRNA using mMessage mMachine<sup>®</sup> *in vitro* transcription kit with SP6 RNA polymerase (Ambion<sup>®</sup>). Pannexin-1 mRNA was injected into *Xenopus laevis* oocytes at a final concentration of 1 µg/µL. Concentration of mRNA was assessed using a NanoDrop<sup>™</sup> 1000 spectrophotometer (Thermo Fisher Scientific). Presence of full-length transcript was confirmed by gel electrophoresis.

### 2.2 *Microinjection of Oocytes*

Defolliculated, stage 5-6 *Xenopus laevis* oocytes were generously supplied to us by Dr. William Zagotta, University of Washington (Seattle, WA). Oocytes were microinjected with 50-80 nL of mPx1 mRNA (1µg/ µL) using a Drummond<sup>®</sup> Digital Microdispenser and incubated at 18°C for 18-36 hours before testing. Oocytes were stored in 12-well culture dishes with standard ND96 media, [in mM]: 96 NaCl, 2 KCl, 1.8 CaCl<sub>2</sub>, 1 MgCl<sub>2</sub>, 5 HEPES with 100 U/mL Penicillin and 100 ug/mL Streptomycin. The medium was changed daily post-injection.

### 2.3 Solutions

Pannexin-1 Control solution [in mM]: 90 NaCl, 2 KCl, 1 MgCl<sub>2</sub>, 3 CaCl<sub>2</sub>, 5 HEPES, pH 7.4. To confirm presence of Px1 current, the Px1 inhibitor, carbenoxolone (CBX, Sigma-Aldrich<sup>®</sup>), was added to this solution to a final concentration of 50 μM.

### 2.4 Two-Electrode Voltage Clamp (TEVC)

Two-electrode recordings were performed with an OC-725C Oocyte Clamp (Warner Instruments) and a Digidata 1440A amplifier (Molecular Devices). Individual oocytes were placed in an acrylic recording chamber and continuously perfused via gravity flow with Pannexin-1 Control solution. Glass capillary microelectrodes (Drummond, #3-000-210-G) were pulled with a vertical PC-10 pipette puller (Narishige, Japan) to a resistance of 0.2-0.3 MΩ and filled with 3 M KCl. Upon entry of the pipette tips into cell membrane, membrane potential was allowed to stabilize for 10-15 minutes before the voltage protocol was applied. Cells were clamped at a holding potential of -40 mV and taken through one of two voltage excursions ranging from 100 mV to +60 mV or -100 to +200 mV in 10 mV or 25 mV steps, respectively. Each voltage-pulse had a duration of 500 milliseconds. After each step-pulse, the membrane potential was returned to resting potential (-40 mV). To confirm the presence of a Px1 current, CBX solution was perfused for 5 minutes before voltage protocols were applied. After CBX application, Px1 Control solution was perfused to wash out CBX as a test of reversibility of CBX inhibition.

## 2.5 *Data Analysis*

Subtractions of currents were performed using AxoGraph X. Tau and Boltzmann fit lines were done with SigmaPlot using equations referenced in this text. Student t-tests were used to perform statistical analyses.

### 3. RESULTS

#### 3.1 Isolation of Px1 current

To investigate Px1 gating as a function of voltage, Px1-injected *Xenopus laevis* oocytes were tested using the two-electrode voltage clamp (TEVC) technique. Applying the voltage protocol illustrated in Figure 3, large currents (1-2  $\mu$ A) were elicited that appear to have some level of voltage-dependence (Fig. 3A, B). Uninjected oocytes were also tested using the same method and yielded current amplitudes less than 300 nA. To further isolate Px1 current from oocyte-specific currents, we used the Px1 inhibiting drug, carbenoxolone (CBX). After treatment with 50  $\mu$ M CBX, approximately 20% of the original current remained (Fig. 3B), suggesting roughly 80% of the original current was current generated by Px1. Px1-resistant current (Fig. 3B) was subtracted from the original current (Fig. 3A) to yield isolated Px1 current for further gating analysis (Fig. 3C). Isolated Px1 currents exhibited characteristic small currents (<100 nA) from -100 mV to 0 mV, and then a marked increase in current amplitude from 0 mV to +60 mV (Fig. 4). We also saw an average reversal potential that was  $1 \pm 5$  mV. From isolated Px1 current-voltage patterns (I-V), Px1 channels seemed to be closed at negative voltages, and showed outward rectification at voltages >20 mV.

#### 3.2 Voltage-dependence of Px1 currents

Px1 seemed to have some level of voltage dependence based on rectification seen in the I-V patterns; however, current (I) is generated by two main components as shown in the following equation:

$$I = G(V - V_{rev}) \quad (\text{Equation 2})$$

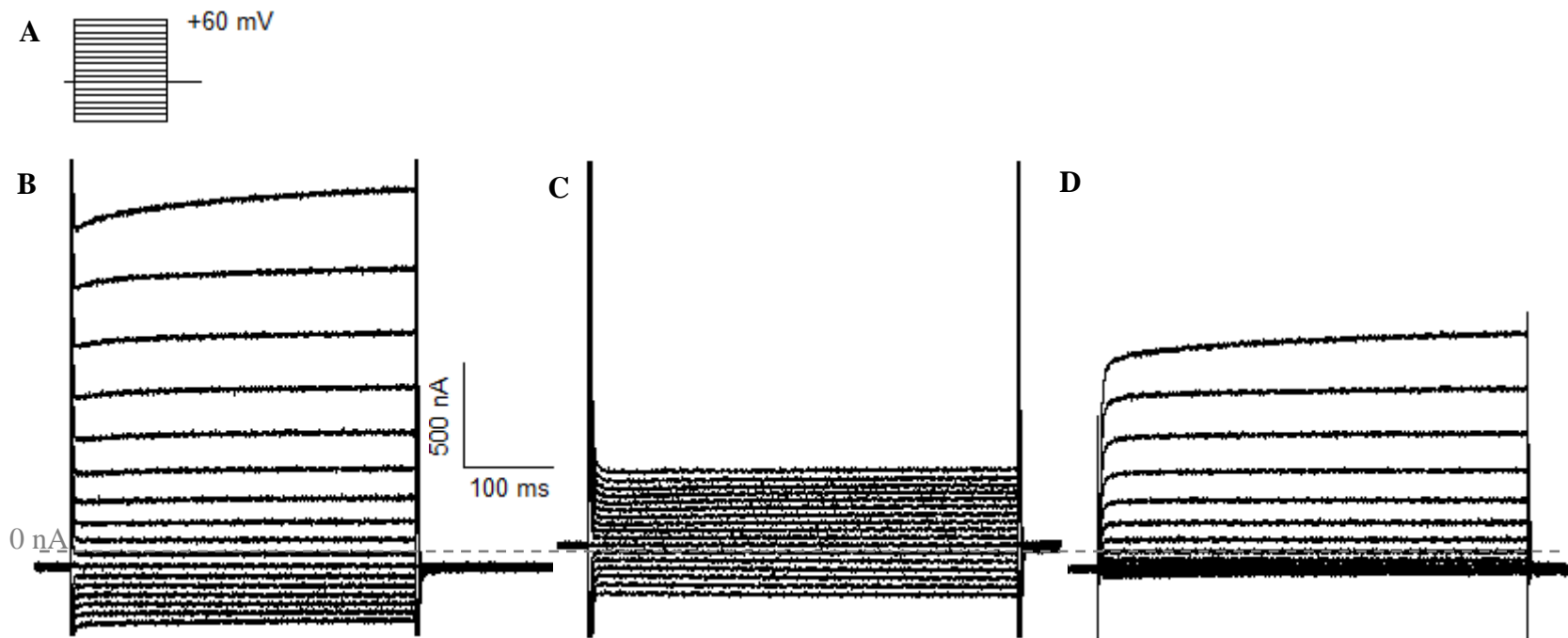


**Figure 3.** Pharmacological isolation of Px1 current. **A**, Voltage protocol ranging from +60 mV to -120 mV used with TEVC. Clamped oocytes were held at a resting potential of -40 mV. **B-D**, Current traces recorded from *Xenopus laevis* oocytes either injected with 80 ng of mPx1 mRNA (c,d), or uninjected (b) using TEVC mode. **B**, Voltage-dependence was seen by unequal current responses to various voltages. **C**, 50 μM CBX-insensitive current shown in Px1-injected oocyte. **D**, subtraction of ‘CBX-insensitive’ current from ‘Px1-injected’ revealed CBX-sensitive current, or ‘isolated Px1’ current.

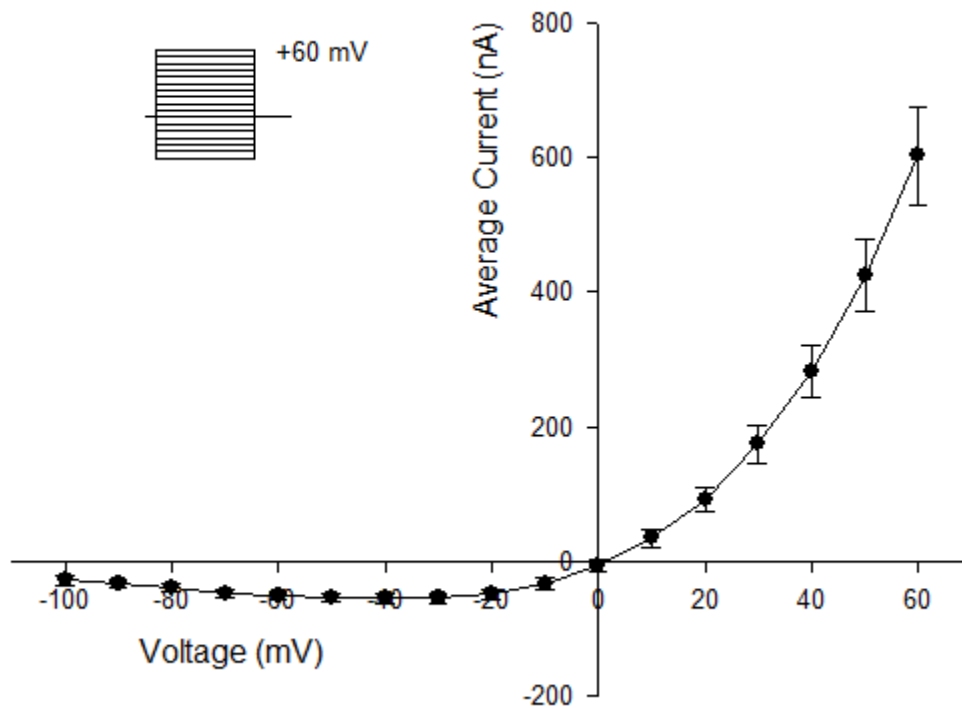


**Figure 4.** Current-voltage (I-V) relationship of Px1 with +60 mV protocol. Values are given as means  $\pm$  SEM, n=22.



in which  $G$  is conductance, and  $V_{rev}$  is the reversal potential. The first component,  $G$ , is proportional to  $NP_o\gamma$ , where  $N$  is the number of channels,  $P_o$  is the open probability of each channel, and  $\gamma$  is the unitary conductance of each channel. The second component,  $V-V_{rev}$ , is a measure of the driving force created by electrochemical gradients present at the time of channel opening. To separate driving force (permeation) from intrinsic voltage-dependent properties of Px1 channel opening (gating), we calculated  $G$  according to equation 3, and plotted normalized conductance ( $G/G_{max}$ ) values as a function of voltage (Fig. 5).

$$G = \frac{I}{(V-V_{rev})} \quad (\text{Equation 3})$$

At voltages between -100 and +60 mV, conductance seemed to be continually increasing, suggesting Px1 did not approach maximal opening at these voltages. We thus extended the voltage protocol to +200 mV, at which Px1 current increased 2- to 5-fold compared to activation at +60 mV. Plotting  $G/G_{max}$  values as previously described, relative conductance seemed to reach a plateau, indicating maximal opening of Px1 channels started at approximately +150 mV (Fig. 6). Fitting average normalized G-V values with the Boltzmann equation (Equation 4),  $V_{0.5}$ , or the voltage at which half-maximal activation occurred, was calculated to be  $51 \pm 8.3$  mV, with a slope factor  $k = 35.2 \pm 2.9$  mV.

$$I V = \frac{G(V-V_{rev})}{1+e^{-\frac{(V_{0.5}-V)}{ka}}} \quad (\text{Equation 4})$$

### 3.3 Activation Kinetics of Px1

No differences in activation rates were observed at voltages up to +60 mV (not shown), so we utilized the extended voltage protocol to +200 mV to characterize activation kinetics as well.

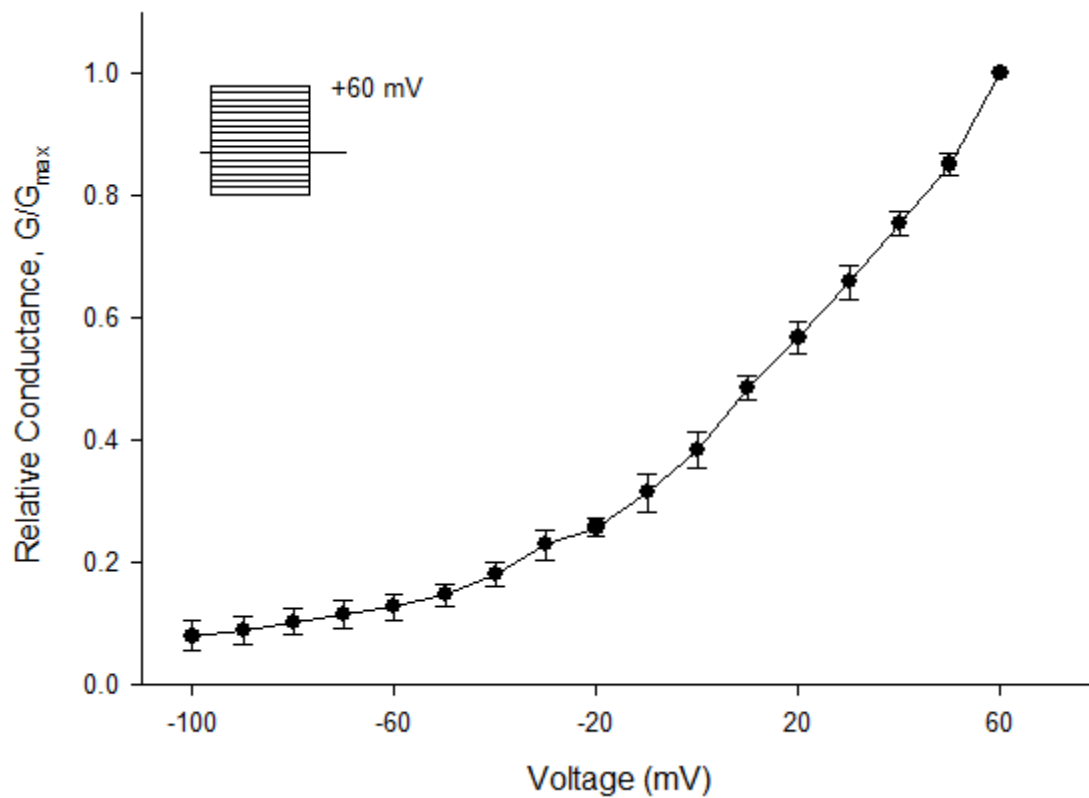


**Figure 5.** Activation curve of Px1 with +60 mV protocol. Average normalized conductance-voltage relations. Values are given as means  $\pm$  SEM, n=22.

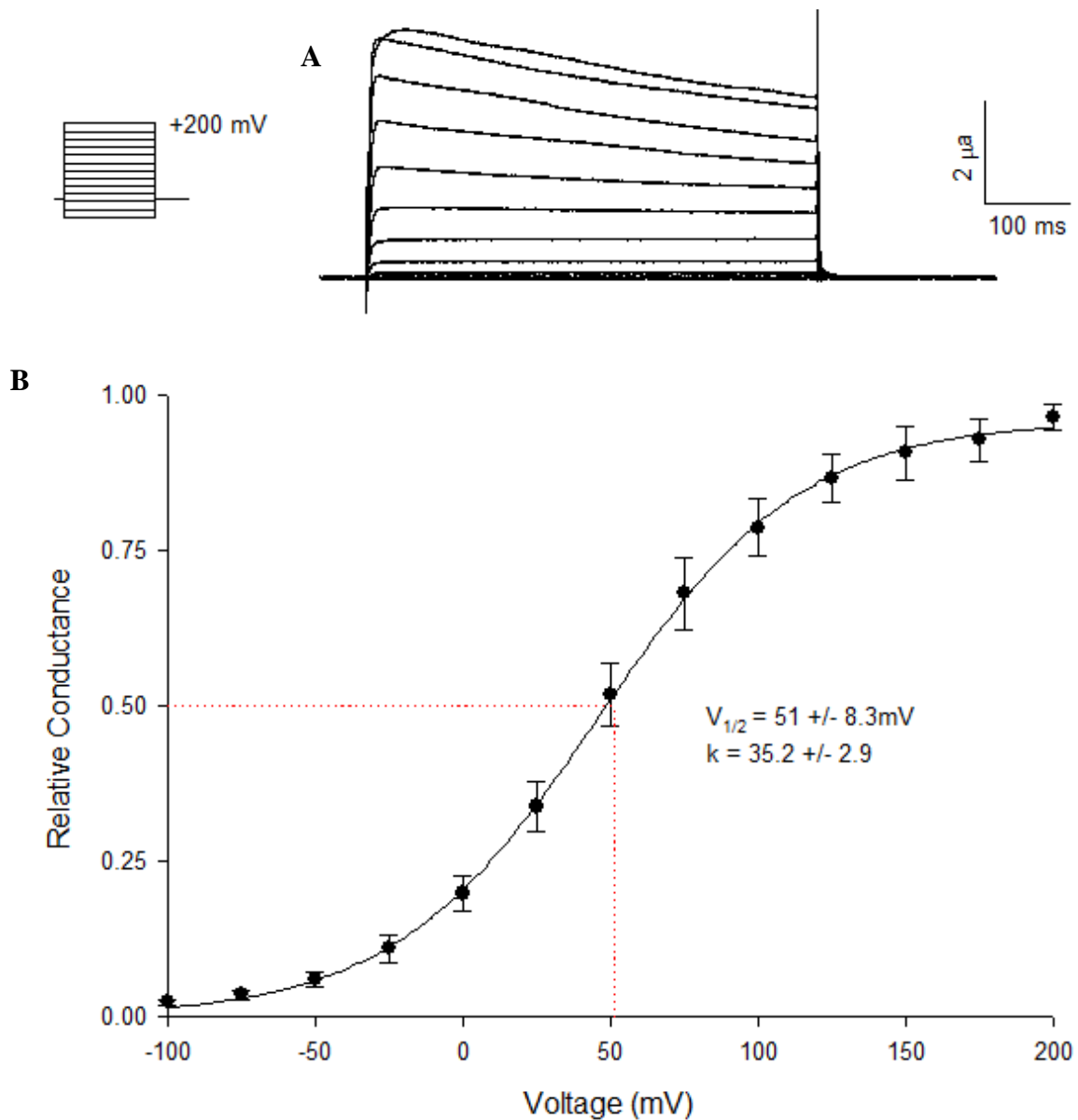


**Figure 6.** Px1 current and activation curve with +200mV protocol. **A**, isolated Px1 current traces using +200 mV protocol. **B**, Average normalized conductance-voltage relations fit with Boltzmann equation as described in Materials and Methods. Px1 maximal activation shown by presence of plateau with extended voltage protocol to +200 mV. Values are given as means  $\pm$  SEM, n=8.

The rising phases of isolated Px1 currents (Fig. 7A, inset) were normalized to peak values at +150 mV. These values were then averaged and superimposed to visually demonstrate differences in activation rate (Fig. 7b). Normalized 100mV and 50mV currents showed no visible difference, so for clarity only 150 and 50mV are shown for comparison. Isolated Px1 current traces at 175 and 200mV were not used for analysis due to a large increase in oocyte-specific currents. Average normalized current data (Fig. 7b) were fitted using a single-exponential function (equation 5) to estimate the time constant of activation ( $\tau_{act}$ ).

$$f(t) = 1 + a_1 e^{-t/\tau_{act}} \quad (\text{Equation 5})$$

Time constants of activation for 150, 100, and 50mV were estimated to be 2.4 +/- 0.3ms, 3.0 +/- 0.3ms, and 3.5 +/- 0.3ms, respectively (Fig. 7c). Though differences in  $\tau_{act}$  were small, Px1 activated 20% and 26% faster at 150mV than 100mV and 50mV, respectively. Differences in  $\tau_{act}$  at 150mV and 50mV were found to be significant ( $p < 0.05$ ), using a student t-test.

### 3.4 Large oocyte-specific current elicited at high voltages

When examining currents elicited by the +200mV protocol, we noticed an apparent level of inactivation at higher voltages (Fig. 9). However, we also noted that there seems to be a decrease in CBX inhibition of currents at higher voltages, particularly at steady state (late current). To investigate whether the apparent inactivation could be an artifact of potential decreased CBX efficacy, we compared the %CBX block at low vs. high voltages (Fig. 8A), as well as compared CBX-resistant current traces from both Px1-injected and uninjected oocytes (Fig. 8B, C). The %CBX block was calculated by dividing isolated Px1 current (net

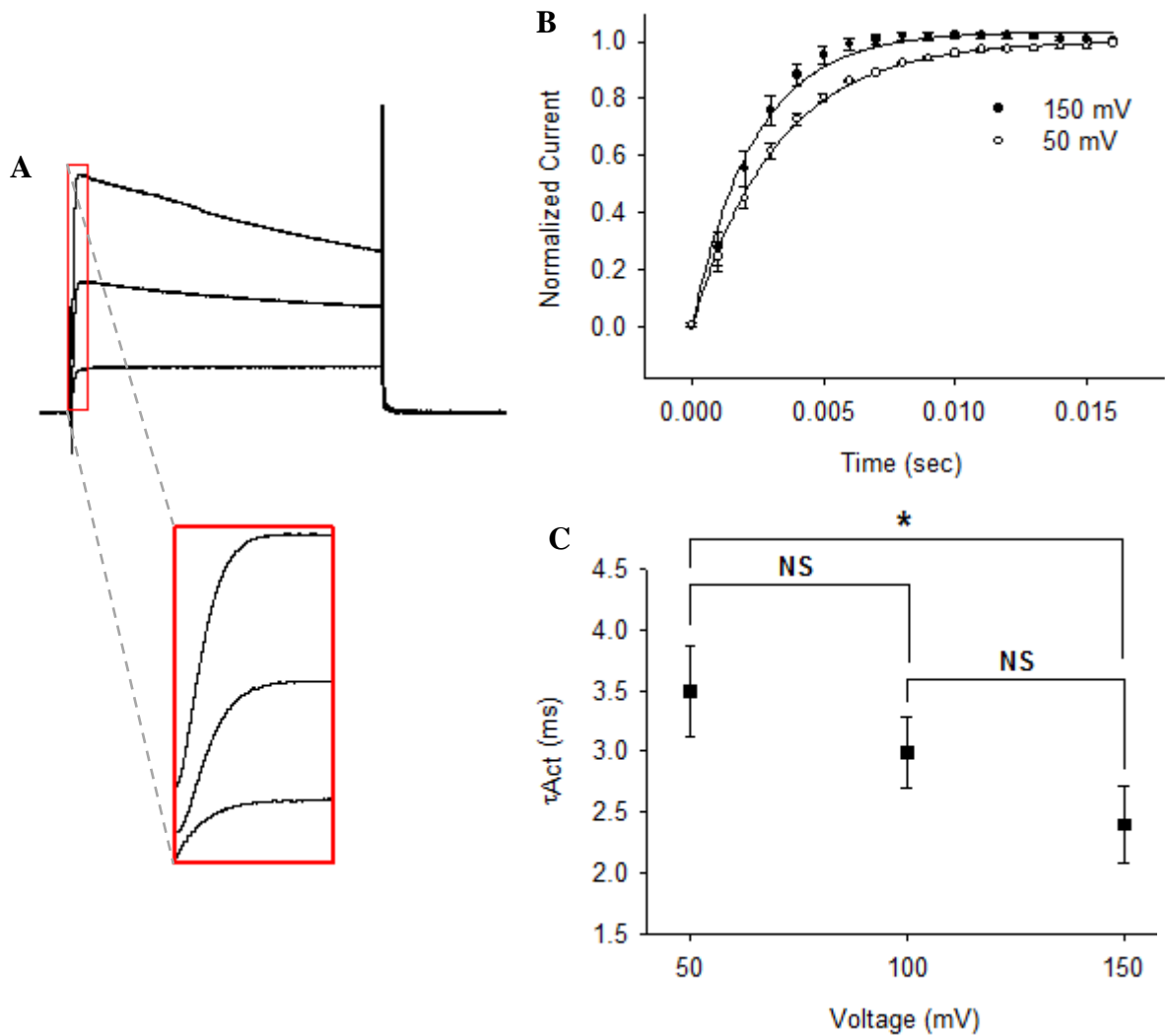


**Figure 7.** Activation rates of Px1 at 150mV, 100mV, and 50mV. **A**, Rates were calculated by fitting simple two- or three-component exponentials to current sections ranging from initial rise phase to peak (inset). Exponentials were fitted using SigmaPlot. **B**, Normalized current sections were superimposed to visually demonstrate differences in activation rate at 150 mV and 50 mV. 100 mV and 50 mV were almost identical; for clarity of presentation, normalized 100mV trace is not shown. **C**, Time constants calculated for 150 mV, 100 mV, and 50 mV. Values are given as means  $\pm$  SEM, n=8. Significance was determined using student t-test (\* $p < 0.05$ ).

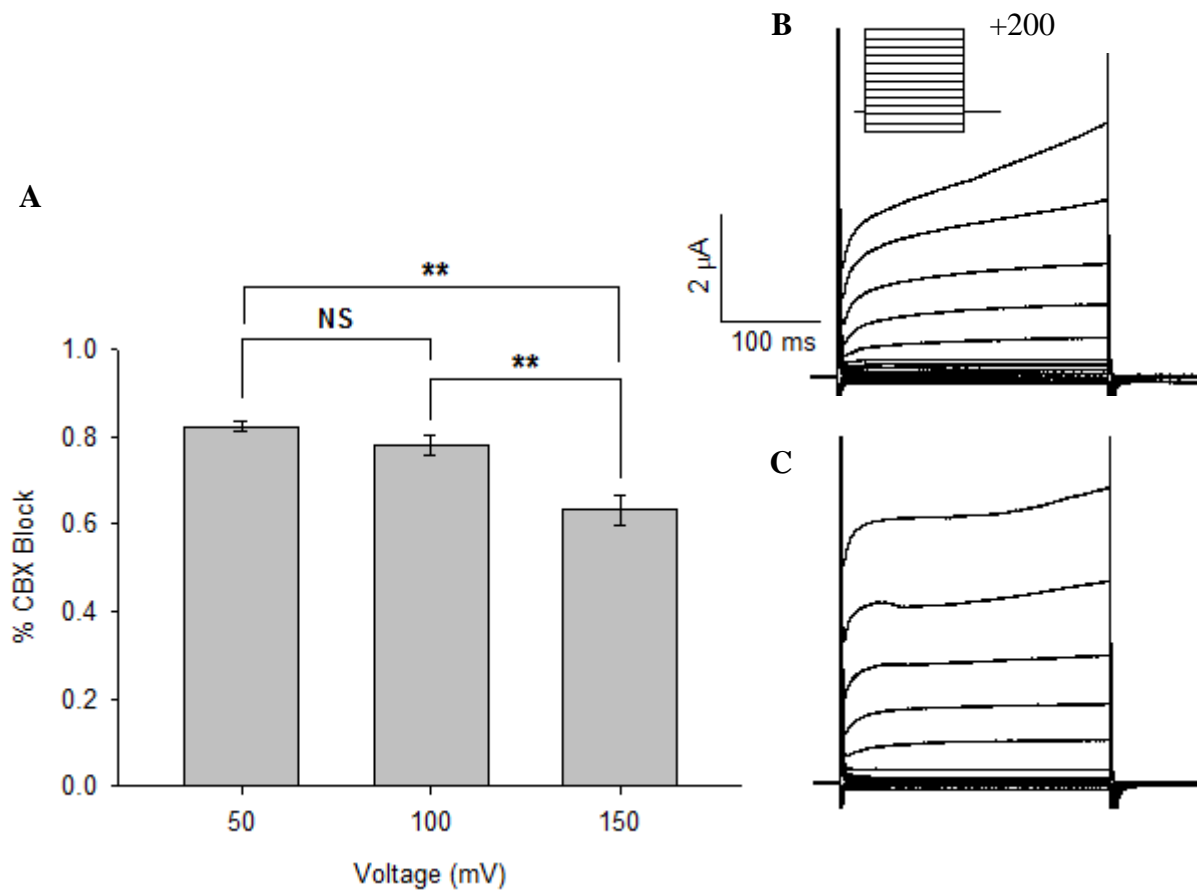


**Figure 8.** Oocytes exhibited increased outward current at high voltages. **A**, Percent CBX block of Px1 in injected oocytes showed an apparent decrease at voltages >100mV. **B-C**, Uninjected oocyte current with 50uM CBX (**B**) showed similar kinetics and shape to Px1 injected oocyte current with 50uM CBX (**C**). Values are given as means  $\pm$  SEM, n=8.

current as described previously) by original current amplitudes at +150, 100, and 50 mV, yielding averages of 63.2 +/- 3.4%, 78.0 +/- 2.2%, 82.4 +/- 1.2%, respectively. Though statistical differences were found between the %CBX block for t-test comparisons at [+50 mV, 150 mV;  $p < 0.001$ ] and [100 mV, 150 mV;  $p < 0.001$ ], comparisons between ‘Px1-injected + CBX’ and ‘uninjected + CBX’ current traces (Fig. 8B, C) showed similar kinetics and shape, suggesting that the apparent decrease in CBX efficacy can likely be attributed to the exaggerated increase in endogenous oocyte currents at high voltages. Comparing control cells using the same +200 mV voltage protocol, oocytes seemed to express endogenous channels that were activated at high voltages >75 mV. Further, CBX showed marginal (< 10%) change in these oocyte-specific currents, suggesting that the isolated Px1 currents at high voltages were predominantly attributable to Px1, and that the apparent decrease in %CBX inhibition was likely due to an increase in steady-state (late) current from endogenous oocyte channel populations. Therefore, we proceeded to examine the level of Px1 inactivation at high voltages.

### 3.5 Current Decay of Px1

To detect whether current decay (CD) occurs in Px1, we divided current amplitudes at 500ms ( $I_{500ms}$ ) by peak current amplitudes ( $I_{peak}$ ). Currents shown in Figure 9A displayed a peak to 500 ms for +150, 100, and 50 mV traces; respective CD ratios were calculated to be 0.71 +/- 0.05, 0.86 +/- 0.05, and 1.05 +/- 0.06. CD ratios (Fig. 9B) showed a decreasing  $I_{peak}/I_{500ms}$  ratio with increasing voltage, suggesting that CD was more prevalent at higher voltages. No significant differences were found between  $I_{peak}/I_{500ms}$  at 100 and 150mV, however,  $I_{peak}/I_{500ms}$  between [50, 100 mV] and [50, 150 mV] were found to be significant (p

<0.05,  $p < 0.001$ , respectively). Therefore, our data suggests Px1 currents exhibit current decay at high positive voltages.



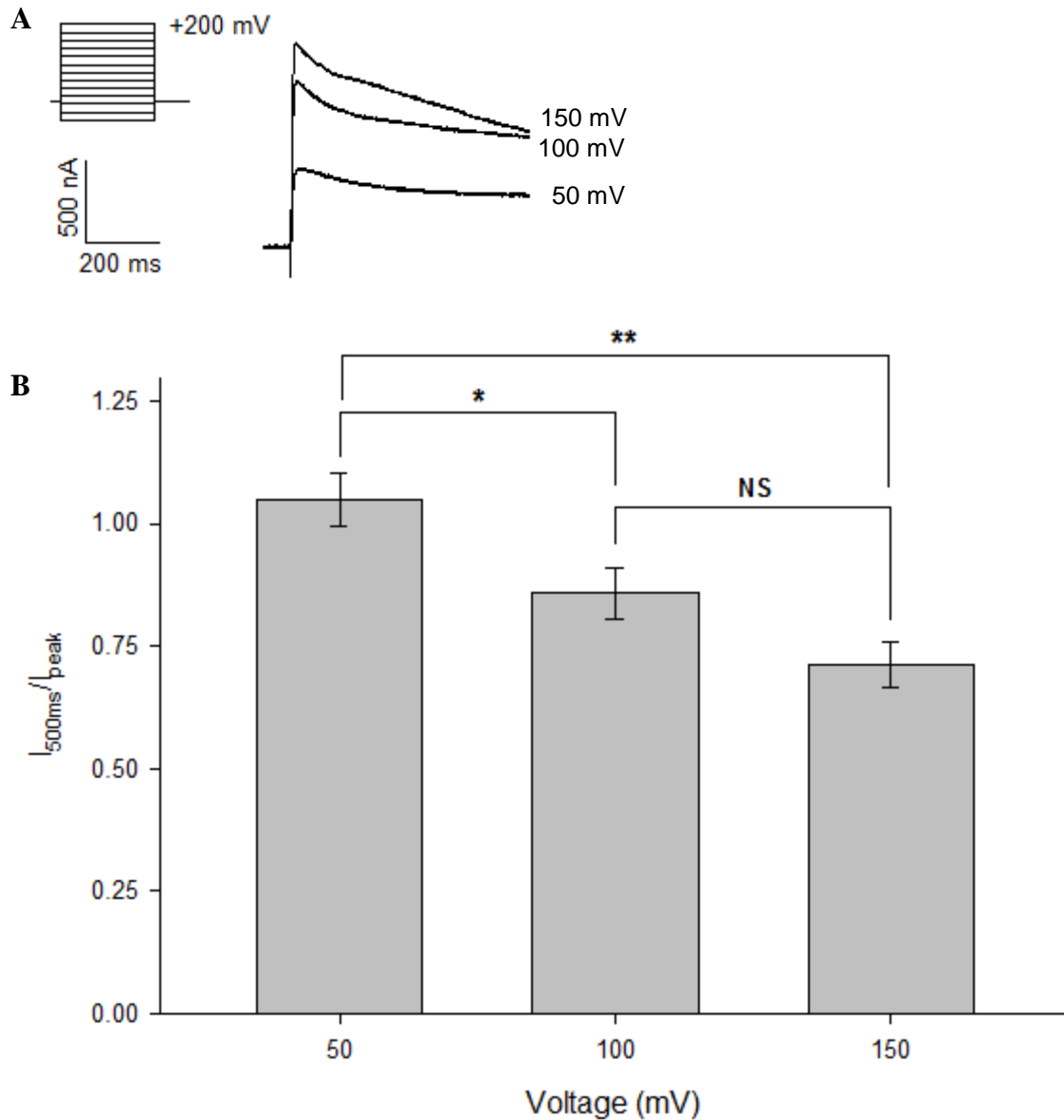


**Figure 9.** Isolated Px1 current showed slow current decay. **A**, Current traces at +150 mV, 100 mV, and 50 mV. CD ratios were calculated by dividing  $I_{500ms}$  by  $I_{peak}$ . **B**,  $I_{500ms}/I_{peak}$  ratios measured at +150 mV, 100 mV, and 50 mV. Significant differences between indicated pairs determined by student t-tests, \* $p < 0.05$ , \*\* $p < 0.001$ . Values given are means  $\pm$  SEM,  $n=8$ .

## 4. DISCUSSION

In the present study, we investigated previously uncharacterized gating properties of the Pannexin-1 channel. Prompted by previous accounts of Px1 being a voltage-dependent channel, we plotted normalized conductance values against voltage, and discovered that Px1 reaches maximal activation at voltages  $\geq +150$  mV. For the first time, we have shown Px1 Boltzmann activation parameters, redefining Px1 as a weakly voltage-gated channel. Further, through kinetic analysis, we have identified Px1 activation rates ( $\tau_{\text{act}}$ ) at half-maximal and maximal activation voltages, uncovering fast and weakly voltage-dependent activation kinetics of Px1. Additionally, we noticed a consistent current decay at high positive voltages, which we hypothesize to be indicative of either inactivation or entrance of Px1 into a sub-conductive state(s). We also noticed a short ( $> 24$  hrs) window of Px1 expression in both *Xenopus laevis* oocytes and the mammalian Neuro2a cell line (data not shown). Taken together, the results of our study portray Px1 to be a very tightly regulated, if not ‘reluctant,’ channel.

### 4.1 *Px1 is a voltage-sensitive channel*

Gating of a channel can occur in many different ways; however, voltage-dependent gating relies on conformational changes in protein structure brought about by shifts in membrane voltage ( $V_m$ ). Voltage-sensing domains (VSD) containing select charged or polar residues that respond readily to changes in membrane potential translate small conformational changes in subunit tertiary structure to open the ‘gate’ of a channel, thus permitting ion access to the pore. This study was prompted by Px1 current-voltage relationships (I-V) that suggested some level of voltage-dependent activation, exhibiting an

apparent current threshold, with minimal current amplitudes at negative voltages and increased current amplitudes at positive voltages. Also, Px1 currents showed large outward rectification, or graded, unequal increases in current amplitude with increasing voltages  $> +20$  mV. Visual inspection of current traces and current-voltage relationships has previously been the only way that Px1 has been characterized in terms of voltage-dependence (Bruzzone et al., 2003). To quantitatively evaluate voltage-dependent activation specific to Px1, it was necessary to isolate changes in conductance that are a consequence of the channel itself, and not of the driving force. Equation 2 shows that current (I) is generated by both conductance (G) as well as the driving force ( $V - V_{rev}$ ); by dividing current by the driving force, we isolated intrinsic properties of the channel, since  $G = NP_o\gamma$  (see equation 2). By plotting normalized conductance values ( $G/G_{max}$ ) against voltage (V) as in Figure 6B, we showed that Px1 was maximally activated at voltages higher than +120 mV, and had a Boltzmann fit slope  $k = 35$  mV. This large slope suggested very weak voltage-dependence, as large increases in voltage were required to further activate the channel. Strongly voltage-dependent channels such as select  $K^+$  and  $Na^+$  channels are fit with much smaller slope values, illustrating greater voltage-sensitivity through a steeper slope (Table 1). The large slope for Px1 activation by voltage can be compared to the temperature- and voltage-dependent TRPM4 channel, which is also considered to be weakly voltage-dependent (Nilius et al., 2005).

**Table 1.** Boltzmann parameters of select voltage-gated channels.

	$V_{0.5}$ (mV)	$k_a$ (mV)
Pannexin-1	51 $\pm$ 8.3	35.2 $\pm$ 2.9
TRPM4 <sup>1</sup>	92	32
Kv3.3 <sup>2</sup>	19.5 $\pm$ 0.3	9.4 $\pm$ 0.2
Kv4.3 <sup>3</sup>	-7.9	12.34

<sup>1</sup> (Nilius et al., 2005); <sup>2</sup> (Minassian et al., 2012); <sup>3</sup> (Patel et al., 2004)

Though it has been suggested that voltage alone can open Px1 (Thompson et al., 2008a), there seem to be other voltage-independent ways of opening Px1. Cleavage of the C-terminus of human Px1 (hPx1) by caspase induces current from Px1 independent of voltage, and thus has been shown to be sufficient to open Px1 (Sandilos et al., 2012), however Px1 currents still retain voltage-sensitivity. Therefore, a re-thinking of Px1 as being solely a ‘voltage-dependent’ channel is required. We propose that while currents generated by Px1 seemed to have voltage-dependent qualities, the channel itself seems more appropriately termed ‘voltage-sensitive,’ as its gating seems not to rely only on changes in voltage; further, our data suggests Px1 is weakly gated by voltage alone. While hPx1 can be opened simply by caspase cleavage, it seems that truncated hPx1 current still retains similar voltage-sensitivity with increasing depolarizations, as caspase-induced cleavage of the C-terminus produced an I-V relationship almost identical to intact hPx1 in Jurkat cells, with little current at negative voltages, and graded current increases at depolarizing voltages. Differences between C-terminally truncated hPx1 and mPx1 were minimal, however hPx1 showed more of a decrease in current at hyperpolarizing voltages (Sandilos et al., 2012).

It is still unclear if cleavage of the Px1 C-terminus is necessary to activate Px1, or if this potential C-terminal gating mechanism may operate separate from, or in conjunction with, voltage-gating. Additionally, since changes to Px1 voltage-sensitivity are not immediately apparent through visual inspection of I-V relationships, it is possible that the residues conferring voltage-sensitivity to Px1 are not located in the C-terminus. Due to similarities in currents elicited from caspase-cleaved hPx1 and mPx1 (Sandilos et al., 2012), and that many C-terminal residues were determined to be in the mPx1 pore through substituted cysteine accessibility method (SCAM) analysis (Wang and Dahl, 2010), it is

possible that gating residues may be present in the C-terminus of mPx1. Further, it seems that residues that confer voltage-sensitive activation of mPx1 are not located in the C-terminus. It is worth investigating the role of caspase cleavage in conjunction with studies of activation rate and Boltzmann activation curves to identify differences, if any, in activation once C-terminal cleavage occurs. Further investigating these properties of Px1 could be very helpful in determining selective treatments for immune disorders or neurological (voltage-mediated) conditions.

Identifying Px1 as a voltage-sensitive channel is consistent with current published data, and we consider it to be a more accurate portrayal of the role voltage plays in Px1 gating. It is possible that Px1 voltage-sensitivity could be governed or altered by other mechanisms that have yet to be investigated, or may be coordinated by initial cleavage of the C-terminus by caspase. The new findings we present here may aid in identification of other, perhaps allosterically regulated, modes of Px1 gating.

#### *4.2 Activation of Px1*

In order for a channel to be sensitive to voltage, there must be present in the structure of the protein charged or polar residues that can effectively respond to changes in membrane potential and influence the structure or availability of the pore. Though the crystal structure of Px1 has not yet been determined, SCAM analyses have led to predictions of pore-lining residues, and key components to channel activity in intracellular/extracellular domains have been proposed (Wang and Dahl, 2010). It seems that multiple C-terminal residues are modified by thiol reagents indicating potential presence in the pore. Serial deletion experiments showed that the C-terminus is required for Px1 inhibition, which might indicate

a possible gating mechanism intrinsic to the Px1 C-terminus (Sandilos et al., 2012). This is consistent with the aforementioned evidence of Px1 activation by caspase cleavage (Wang and Dahl, 2010; Sandilos et al., 2012). Further, C346S mutation generated Px1 channel that has increased current at all voltages, which might be an indicator that this particular residue plays a key role in Px1 inhibition (Wang and Dahl, 2010; Bunse et al., 2010).

Our G-V data suggested that there is some level of voltage-dependence intrinsic to Px1 channels. Px1 is a multimeric protein, composed of six four-transmembrane monomers. Based on studies of other voltage-dependent channels, the voltage-dependent changes in Px1 current are theoretically due to conformational changes of the channel caused by protein-protein interactions between Px1 subunits. Though there are multiple ways to trigger cooperative movement of monomers in multimeric membrane proteins (ligand binding, mechanosensitivity, etc.), the changes we showed in the present study were due to changes in voltage. Voltage-sensitive constituents of a channel are typically charged or polar residues that are affected by shifts in membrane voltage ( $V_m$ ). In turn, changes in  $V_m$  can confer overall conformational modifications to the channel, thus allowing opening, closing, or inactivation to occur. These voltage-sensing regions have been illustrated through x-ray crystallographic studies of many well-documented channels to document a variety of voltage-sensing domains.

The slope determined by the Boltzmann fit of Px1 activation is related to the number of charges required to move in order to open the channel (Table 1). A large slope implies low level of gating charges present, minimal contribution to channel opening conferred by said charges, or a combination of both. Thus, large inputs of voltage are necessary to create measurable changes in channel opening or to increase channel open probability. Consistent

with data shown in Table 1, K<sup>+</sup> channels generally have steep activation slopes (low k value in Boltzmann fit of activation curve) and also typically have arginine-rich domains, which assume the role of a canonical ‘voltage-sensor’ in K<sup>+</sup> channels. Voltage-sensing domains of ion channels are dense with charged residues that allow sections of the protein to respond readily to changes in membrane voltage. There are no domains of Px1 that are immediately apparent as voltage-sensors, which is consistent with our findings that Px1 is a weakly voltage-gated channel (shown by the activation curve in Figure 6B).

Charge-dense regions are not required to confer voltage-sensitivity to a channel, however. A recent study showed that altering one residue conferred voltage-dependence to a channel that lacked a canonical ‘voltage-sensing domain’ (Kurata et al., 2010). The Px1 relative, Connexin43, also lacks a canonical VSD, though neutralization of one charged residue in the C-terminus changed voltage-dependent junctional gating, and neutralizing two charged residues eliminated all voltage-dependent junctional gating (Revilla et al., 2000). Connexin26 (Cx26), also seems to lack a canonical voltage sensor, though it displays voltage-dependent activation as well (González et al., 2006), suggesting that voltage-sensitivity without a traditional voltage-sensor is plausible in Px1.

SCAM analyses have provided preliminary estimates for locations of crucial residues in the membrane, though without the crystal structure of Px1, only inferences can be made about key voltage-sensing residues. As previously mentioned, it seems the C-terminus of Px1 might play a role in initial gating of Px1, though this has only been shown through C-terminal cleavage by either caspase or other proteases *in vitro* (Sandilos et al., 2012). It is unclear whether truncation or other structural modifications to the C-terminus are necessary to gate Px1, however, removal of the C-terminus does not seem to eliminate voltage-

sensitivity of Px1. From this, we can predict that residues contributing to Px1 voltage-sensitivity are not present in the C-terminus, but further studies are required to determine key voltage-sensitive residues. Considering the weak voltage-sensitivity of Px1 shown in this study, it is likely that there are either relatively few gating charges present (as opposed to a VSD), or that the charges present contribute minimally to gating as a response to voltage. To determine these features of Px1 in future studies, the protein structure must be solved in order to identify key voltage-sensing residues.

In Figure 7, we show asymmetric increases amplitude and also speed (activation rate,  $\tau_{act}$ ) of Px1 currents with increasing voltages. Activation of channels in general requires transient modifications to protein structure to allow access to the pore from one or both sides of the membrane. Px1 is thought to be a hexameric channel composed of six four-transmembrane proteins with a large intracellular loop and intracellular N- and C-termini (Fig. 10). Access to the pore is likely permitted by charged residues in the protein that, with increasingly positive voltage conditions, undergo slight alterations to tertiary structure of the Px1 monomers, which can cooperatively affect quaternary structure of the Px1 hexamer.

Though large increases of voltage were necessary to elicit maximal channel opening as shown in Figure 6B, the rate at which Px1 opens seemed to remain relatively unchanged with increasing voltages (Fig. 7B). Px1 seemed to show high cooperativity between subunits based on fast activation rates, however, the small changes in  $\tau_{act}$  suggest this cooperativity was very weakly voltage-sensitive; it is still possible, however, that additional protein modifications can modulate this parameter. Though the rate of activation did seem to increase by approximately 26%, compared to channels that have very strong voltage-dependent activation rates, such as Na<sup>+</sup> channels that exhibit logarithmic increases in



activation rates, our data suggests that Px1 activation rates are weakly voltage-sensitive, consistent with our G-V data showing limited voltage-sensitivity.

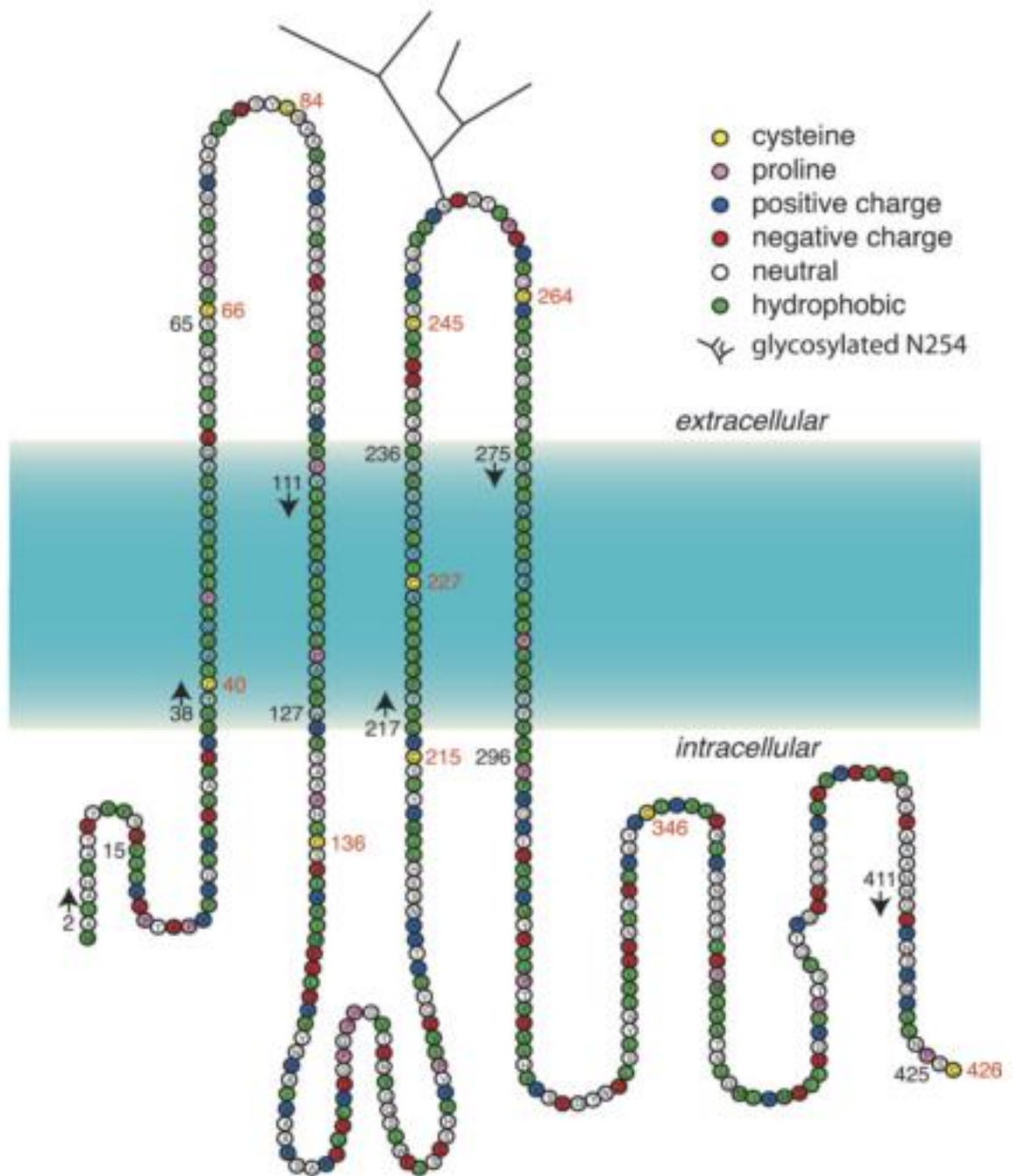


**Figure 10.** Proposed arrangement of Px1 monomer (Wang and Dahl, 2010). Charged residues are indicated in blue and red.

### 4.3 *Current decay of Px1*

We showed that Px1 appeared to display decaying currents at higher voltages and long depolarizations, though further investigation is necessary to determine whether current decay is due to decreasing availability of Px1 channels (inactivation) or entrance into a subconductive state. Single channel experiments have shown that Px1 does have multiple subconductive states at +60 mV, so it is certainly possible that this may be the case (Bao et al., 2004). Connexins display a subconductive state that resembles macroscopic inactivation (Boassa et al., 2007). Since Pannexins and connexins have been found to be topologically and functionally similar, it seems plausible that Px1 could display similar behavior at high positive voltages. No inactivation seems to be present, however, at lower voltages. Perhaps this could be interpreted as a lack of subconductive states at lower voltages, or a lack of inactivation due to low open probability at +60 mV. Single-channel experiments must be done to decipher whether the decreasing current at high voltages is due to subconductive states or rather a voltage-dependent inactivation. For the purposes of analysis, there are three primary hypotheses for the apparent inactivating current seen in Px1.

One possibility is state-dependent inactivation, or inactivation that is reliant on another state to occur. For example, some channels must be open in order to undergo inactivation response, such as sodium channels. Na<sup>+</sup> channels have well-documented accounts of open-state inactivation, where inactivation is reliant on prior opening of the channel (Armstrong and Bezanilla, 1977; Groome et al., 2011). So, if a channel is more likely to be open at a certain voltage (i.e., higher open probability), the channel is then more likely to inactivate. Because Px1 only reaches maximal activation at voltages higher than 100 mV, then inactivation would be unlikely to occur unless those voltages are reached. This

explanation fits with our data showing maximal opening of Px1 channels at high positive voltages. At +60 mV, no inactivation has been detected, and perhaps it is because +60 mV is only approximately the voltage at half-maximal activation (Fig. 6B).

Another option is that Px1 has an intrinsic voltage-dependent inactivation state, which is only triggered at voltages  $>+100$  mV. The Cav1.2 calcium channel exhibits voltage-dependent inactivation, whereby the C-terminus is a crucial part of regulating voltage-dependent inactivation (Cohen-Kutner et al., 2012). The C-terminal region of the Cav1.2 channel acts as a binding domain for the regulatory molecule calcineurin, which negatively regulates inactivation at low positive voltages. Considering data regarding potential regulatory domains of Px1 suggested by constitutive opening of the channel through cleavage of the C-terminus, the question arises about the role of the C-terminus in gating Px1. In future studies, investigating presence of Px1 current decay at voltages  $>+100$  mV in conjunction with modifications to the C-terminus could potentially shed light on inactivation possibilities for Px1.

The third possibility is that Px1, like Connexins, displays a macroscopic subconductance state that resembles slow inactivation. Subconductance states occur when a channel is open and conductive, however the conductance is lower than maximal. Connexin26 shows a macroscopic subconductance state at high voltages, and as a relative of these gap junction proteins, it is also plausible that Px1 could display a similar macroscopic subconductive state (González et al., 2006).

#### 4.5 Deactivation

Typically, gating studies include deactivation rates and characterization by using an ‘open I-V’ protocol and measuring tail currents at negative potentials. It is worth mentioning that through our trials we were not able to sufficiently conclude that our data was not contaminated by transient activity in our recordings. Often, current amplitudes are quite large ( $>10 \mu\text{A}$ ), but with Px1, our current amplitudes were only around 1-2  $\mu\text{A}$  for +60 mV. This made it so our transient was large enough to contaminate our deactivation rising phase, making it difficult to isolate Px1-specific activation rates. When attempts were made to plot open-iv current relationships, the reversal potential was extremely positive  $>35 \text{ mV}$ . Considering other data (Ma et al., 2012) and unpublished data from our lab, Px1 seems to be an anionic-selective channel, which would logically have a reversal potential close to that of chloride, or -20 to -30 mV. The prediction we have is that the contribution of transient to this data is such that the observed reversal potential is close to the opening voltage of the protocol in question (i.e., opening channels at +60 mV). This hypothesis was prompted by observed reversal potentials around  $+60 \pm 20 \text{ mV}$ . At this time, we do not feel it is correct to report estimates on closing rates, however, future studies will include using patch clamp experiments, which will provide a more precise means of detecting deactivation kinetics.

#### 4.4 Px1 turnover rate suggests possible regulation mechanism

The availability and expression of Px1 is a unique feature of Px1—this channel has proven to be quite difficult to study not only because of its reluctance to open maximally, but also due to variations in time-dependent expression levels. We consistently observed a drastic decrease in Px1 current amplitudes  $>24$  hours post-injection of mPx1 mRNA into X.

*laevis* oocytes (approximately 300-500 nA, compared to ‘full’ expression levels of 1-2  $\mu$ A), and >18 hours post-transfection with mPx1-eGFP in the mammalian Neuro2a cell line (data not shown). Currents expressed in these cells did retain sensitivity to CBX inhibition (see Figure 6) and displayed similar voltage responses, though smaller current amplitudes produced ‘noisier’ subtractions that were not suitable for analysis of gating. This apparent rapid loss of Px1 functionality gave us a window of testing oocytes of about 12-24 hours post-injection to use cells with the greatest expression levels.

Trafficking studies suggest a long half-life of Px1 that is presumably comparable to P2X<sub>7</sub>R with a half-life of 54 hours (Gehi et al., 2011; Penuela et al., 2007). Functionality of Px1 for the duration of this proposed life-span, however, has yet to be determined. Since application of inhibitors to the secretory pathway revealed slow reduction in cell surface Px1 expression (Penuela et al., 2007), our observations seem contrary to prolonged functional Px1 expression. Because it also seems that the C-terminus is involved in gating of Px1 as well as trafficking to the cell membrane, it is plausible that cleavage or modification to the C-terminus can trigger the endocytic pathway involved in Px1 internalization and degradation (Gehi et al., 2011). Further, the Px1 C-terminus has been found to directly bind F-actin, which is thought to influence cell motility (Bhalla-Gehi et al., 2010), but also could potentially be a step that may render Px1 non-functional as a possible initiation of Px1 endocytosis.

Not much is currently known about the triggers associated with possible endocytosis of Px1 channels, however, it is possible that its diffuse expression could effect slower turnover rates compared to Cx43. Exogenous Px1 expression has shown limited levels of clustering, contrary to the cell surface expression profile of many connexins (Penuela et al.,

2007; Goodenough et al., 1996). This could be a potential reason for the apparent prolonged Px1 surface expression when compared to Cx43; perhaps multiple connexin channels can be targeted for endocytosis at once, where Px1 may undergo more random targeting.

One possibility for decreased Px1 expression over time is simply the exogenous expression in heterologous systems (oocytes and N2a cells). Since this is a large hexameric protein that must be properly assembled in the membrane, it is possible that exogenous expression would be less reliable. However, significantly larger channels, like the cystic fibrosis transmembrane conductance regulator (CFTR)—have been expressed in both systems without any indication of decreased expression over periods of 3-5 days (Serrano et al., 2006). The peculiarity of such a fast loss of function suggests that tight regulation of Px1 is important, and could be a result of intrinsic regulation of Px1 expression levels.

#### *4.5 Conclusion*

We suggest that Px1 is a weakly voltage-gated channel, that displays fast, yet weakly voltage-sensitive activation rates. There is certainly the potential that allosteric regulation of this channel may play a part in Px1 activation, but these aspects are not yet known. It is important to note that in nearly all experiments, Px1 has been tested at voltages at or below +80 mV. We have shown that Px1 is at half-maximal activation at +51 mV, yet Px1 still seems to play a significant role in multiple biological functions even without being maximally activated. Considering involvement of Px1 in seizure-like activity in the hippocampus, ATP signaling, and role in formation of the inflammasome, our data seems to match up with the characteristics of a channel that can play various important biological roles, and logically would be tightly regulated.

As Px1 has such widespread connections to various physiological processes, it is difficult to classify Px1 in terms of supposed function. Px1 has a unique ability to permit fluxes of large polyatomic ions, some cytokines, and various neurotransmitters to the extracellular space, setting it apart from typical ion channels. It is possible that Px1 has diverged from connexins and innexins to assume a role mediating fast purinergic or paracrine signaling. Select small molecules and polyatomic ions that would otherwise be released by slower, vesicular or transporter-mediated mechanisms can pass through the ubiquitously expressed Px1 at much faster rates, allowing more efficient physiological and pathological signaling between cells. With a growing body of evidence supporting fast ATP signaling, it seems fitting that one important role of Px1 is to act as a conduit for fast ATP release (Bao et al., 2004). Further studies about chemically modifying Px1 gating sensitivity could aid in ameliorating Px1-related disease, such as inflammatory bowel diseases, which show decreased Px1 activity in human colon (Diezmos et al., 2013). The link of Px1 to seizure-like activity (Thompson et al., 2008b), neuronal death in response to ischemic stroke (D'hondt et al., 2009; Bargiotas et al., 2011; Thompson et al., 2006), or even its connection to memory formation and synaptic plasticity (Prochnow et al., 2012) make functional characterization of Px1 gating a topic of high importance.

Identifying Px1 as a voltage-sensitive channel is still consistent with current published data, and we consider it to be a more accurate portrayal of the role voltage plays in Px1 gating. It is possible that Px1 voltage-sensitivity could be governed or altered by other mechanisms that have yet to be investigated, but the new findings presented here may aid in identification of other, perhaps more prominent modes of Px1 gating.



## 5. BIBLIOGRAPHY

- Armstrong, C.M., and F. Bezanilla. 1977. Inactivation of the sodium channel. II. Gating current experiments. *J Gen Physiol.* 70:567–90.
- Bao, L., S. Locovei, and G. Dahl. 2004. Pannexin membrane channels are mechanosensitive conduits for ATP. *FEBS letters.* 572:65–8.
- Bargiotas, P., A. Krenz, S.G. Hormuzdi, D. a Ridder, A. Herb, W. Barakat, S. Penuela, J. von Engelhardt, H. Monyer, and M. Schwaninger. 2011. Pannexins in ischemia-induced neurodegeneration. *Proc Natl Acad Sci U S A.* 108:20772–7.
- Bennett, M.V.L., J.M. Garré, J. a Orellana, F.F. Bukauskas, M. Nedergaard, and J.C. Sáez. 2012. Connexin and pannexin hemichannels in inflammatory responses of glia and neurons. *Brain Res.* 1487:3–15.
- Bhalla-Gehi, R., S. Penuela, J.M. Churko, Q. Shao, and D.W. Laird. 2010. Pannexin1 and pannexin3 delivery, cell surface dynamics, and cytoskeletal interactions. *J Biol Chem.* 285:9147–60.
- Billaud, M., J.K. Sandilos, and B.E. Isakson. 2012. Pannexin 1 in the Regulation of Vascular Tone. *Trends Cardiovasc Med.* 22:68-72.
- Boassa, D., C. Ambrosi, F. Qiu, G. Dahl, G. Gaietta, and G. Sosinsky. 2007. Pannexin1 channels contain a glycosylation site that targets the hexamer to the plasma membrane. *J Biol Chem.* 282:31733–43.
- Bruzzone, R., S.G. Hormuzdi, M.T. Barbe, A. Herb, and H. Monyer. 2003. Pannexins, a family of gap junction proteins expressed in brain. *Proc Natl Acad Sci U S A.* 100:13644–9.
- Bunse, S., M. Schmidt, N. Prochnow, G. Zoidl, and R. Dermietzel. 2010. Intracellular cysteine 346 is essentially involved in regulating Panx1 channel activity. *J Biol Chem.* 285:38444–52.
- Chaudhari, N., and S.D. Roper. 2010. The cell biology of taste. *J Cell Biol.* 190:285–96.
- Cohen-Kutner, M., Y. Yahalom, M. Trus, and D. Atlas. 2012. Calcineurin Controls Voltage-Dependent-Inactivation (VDI) of the Normal and Timothy Cardiac Channels. *Sci Rep.* 2:366.
- D'hondt, C., R. Ponsaerts, H. De Smedt, G. Bultynck, and B. Himpens. 2009. Pannexins, distant relatives of the connexin family with specific cellular functions? *BioEssays.* 31:953–74.

- Diezmos, E.F., S.L. Sandow, I. Markus, D. Shevy Perera, D.Z. Lubowski, D.W. King, P.P. Bertrand, and L. Liu. 2013. Expression and localization of pannexin-1 hemichannels in human colon in health and disease. *Neurogastroenterol Motil.* 25:e395-405.
- Gehi, R., Q. Shao, and D.W. Laird. 2011. Pathways regulating the trafficking and turnover of pannexin1 protein and the role of the C-terminal domain. *J Biol Chem.* 286:27639–53.
- González, D., J.M. Gómez-Hernández, and L.C. Barrio. 2006. Species specificity of mammalian connexin-26 to form open voltage-gated hemichannels. *FASEB J.* 20:2329–38.
- Goodenough, D.A., J.A. Goliger, and D.L. Paul. 1996. Connexins, connexons, and intercellular communication. *Annu Rev Biochem.* 65:475–502.
- Groome, J., B. Holzherr, and F. Lehmann-Horn. 2011. Open- and closed-state fast inactivation in sodium channels: Differential effects of a site-3 anemone toxin. *Channels.* 5:57–70.
- Hille, B. 1992. *Ionic Channels in Excitable Membranes.* 2nd ed. Sinauer Associates, Inc. Sunderland, MA. 607 pp.
- Huang, Y.-J., Y. Maruyama, G. Dvoryanchikov, E. Pereira, N. Chaudhari, and S.D. Roper. 2007. The role of pannexin 1 hemichannels in ATP release and cell-cell communication in mouse taste buds. *Proc Natl Acad Sci U S A.* 104:6436–41.
- Iglesias, R., G. Dahl, F. Qiu, D.C. Spray, and E. Scemes. 2009. Pannexin 1: the molecular substrate of astrocyte “hemichannels”. *J Neurosci.* 29:7092–7.
- Kandel, E., and J.H. Schwartz. 1985. *Principles of Neural Science.* 2nd ed. Elsevier Science Publishing Co., Inc. New York, NY. 80 pp.
- Kurata, H.T., M. Rapedius, M.J. Kleinman, T. Baukowitz, and C.G. Nichols. 2010. Voltage-dependent gating in a “voltage sensor-less” ion channel. *PLoS Biol.* 8:e1000315.
- Lai, C.P.K., J.F. Bechberger, R.J. Thompson, B. a MacVicar, R. Bruzzone, and C.C. Naus. 2007. Tumor-suppressive effects of pannexin 1 in C6 glioma cells. *Cancer Res.* 67:1545–54.
- Li, A., and J. Banerjee. 2011. Mechanisms of ATP Release , the Enabling Step in Purinergic Dynamics. *Cell Physiol Biochem.* 28:1135-44.
- Locovei, S., L. Bao, and G. Dahl. 2006a. Pannexin 1 in erythrocytes: function without a gap. *Proc Natl Acad Sci U S A.* 103:7655–9.
- Locovei, S., L. Bao, and G. Dahl. 2006b. Pannexin 1 in erythrocytes: function without a gap. *Proc Natl Acad Sci U S A.* 103:7655–9.

- Locovei, S., J. Wang, and G. Dahl. 2006c. Activation of pannexin 1 channels by ATP through P2Y receptors and by cytoplasmic calcium. *FEBS Lett.* 580:239–44.
- Ma, W., V. Compan, W. Zheng, E. Martin, R.A. North, A. Verkhratsky, and A. Surprenant. 2012. Pannexin 1 forms an anion-selective channel. *Pflügers Arch.* 463:585–92.
- MacVicar, B. a, and R.J. Thompson. 2010. Non-junction functions of pannexin-1 channels. *Trends Neurosci.* 33:93–102.
- Martinon, F., K. Burns, and J. Tschopp. 2002. The inflammasome: a molecular platform triggering activation of inflammatory caspases and processing of proIL-beta. *Mol Cell.* 10:417–26.
- Martinon, F., A. Mayor, and J. Tschopp. 2009. The inflammasomes: guardians of the body. *Annu Rev Immunol.* 27:229–65.
- Minassian, N. a, M.-C. a Lin, and D.M. Papazian. 2012. Altered Kv3.3 channel gating in early-onset spinocerebellar ataxia type 13. *J Physiol.* 590:1599–614.
- Nilius, B., K. Talavera, G. Owsianik, J. Prenen, G. Droogmans, and T. Voets. 2005. Gating of TRP channels: a voltage connection? *J Physiol.* 567:35–44.
- Orellana, J.A., N. Froger, P. Ezan, J.X. Jiang, M.V.L. Bennett, and C.C. Naus. 2011. ATP and glutamate released via astroglial connexin 43 hemichannels mediate neuronal death through activation of pannexin 1 hemichannels. *J Neurochem.* 118:826–840.
- Patel, S.P., R. Parai, R. Parai, and D.L. Campbell. 2004. Regulation of Kv4.3 voltage-dependent gating kinetics by KCHIP2 isoforms. *J Physiol.* 557:19–41.
- Pelegrin, P., and A. Surprenant. 2006. Pannexin-1 mediates large pore formation and interleukin-1beta release by the ATP-gated P2X7 receptor. *The European Molecular Biology Organization Journal.* 25:5071–5082.
- Penuela, S., R. Bhalla, X.-Q. Gong, K.N. Cowan, S.J. Celetti, B.J. Cowan, D. Bai, Q. Shao, and D.W. Laird. 2007. Pannexin 1 and pannexin 3 are glycoproteins that exhibit many distinct characteristics from the connexin family of gap junction proteins. *J Cell Sci.* 120:3772–83.
- Penuela, S., L. Gyenis, A. Ablack, J.M. Churko, A.C. Berger, D.W. Litchfield, J.D. Lewis, and D.W. Laird. 2012. Loss of pannexin 1 attenuates melanoma progression by reversion to a melanocytic phenotype. *J Biol Chem.* 287:29184–93.
- Prochnow, N., A. Abdulazim, S. Kurtenbach, V. Wildförster, G. Dvorientchikova, J. Hanske, E. Petrasch-Parwez, V.I. Shestopalov, R. Dermietzel, D. Manahan-Vaughan, and G. Zoidl. 2012. Pannexin1 stabilizes synaptic plasticity and is needed for learning. *PLoS Biol.* 7:e51767.

- Qiu, F., and G. Dahl. 2009. A permeant regulating its permeation pore: inhibition of pannexin 1 channels by ATP. *Am J Physiol Cell Physiol.* 296:C250–5.
- Revilla, a, M. V Bennett, and L.C. Barrio. 2000. Molecular determinants of membrane potential dependence in vertebrate gap junction channels. *Proc Natl Acad Sci U S A.* 97:14760–5.
- Reyes, J.P., C.Y. Hernández-carballo, G. Pérez-flores, P. Pérez-, and J. Arreola. 2010. NIH Public Access. 380:50–53.
- Sandilos, J.K., Y.-H. Chiu, F.B. Chekeni, A.J. Armstrong, S.F. Walk, K.S. Ravichandran, and D. a Bayliss. 2012. Pannexin 1, an ATP release channel, is activated by caspase cleavage of its pore-associated C-terminal autoinhibitory region. *J Biol Chem.* 287:11303–11.
- Serrano, J.R., X. Liu, E.R. Borg, C.S. Alexander, C.F. Shaw, and D.C. Dawson. 2006. CFTR: Ligand exchange between a permeant anion ([Au(CN)<sub>2</sub>]<sup>-</sup>) and an engineered cysteine (T338C) blocks the pore. *Biophys J.* 91:1737–48.
- Silverman, W.R., J.P. de Rivero Vaccari, S. Locovei, F. Qiu, S.K. Carlsson, E. Scemes, R.W. Keane, and G. Dahl. 2009. The pannexin 1 channel activates the inflammasome in neurons and astrocytes. *J Biol Chem.* 284:18143–51.
- Thompson, R.J., M.F. Jackson, M.E. Olah, R.L. Rungta, D.J. Hines, M.A. Beazely, J.F. Macdonald, and B.A. Macvicar. 2008a. Activation of Pannexin-1 Hemichannels Augments Aberrant Bursting in the Hippocampus. *Science.* 322:1555–1559.
- Thompson, R.J., M.F. Jackson, M.E. Olah, R.L. Rungta, D.J. Hines, M.A. Beazely, J.F. MacDonald, and B.A. MacVicar. 2008b. Activation of pannexin-1 hemichannels augments aberrant bursting in the hippocampus. *Science.* 322:1555–1559.
- Thompson, R.J., and B.A. MacVicar. 2008. Connexin and pannexin hemichannels of neurons and astrocytes. *Channels.* 2:81–6.
- Thompson, R.J., N. Zhou, and B. a MacVicar. 2006. Ischemia opens neuronal gap junction hemichannels. *Science.* 312:924–7.
- Wang, J., and G. Dahl. 2010. SCAM analysis of Panx1 suggests a peculiar pore structure. *J Gen Physiol.* 136:515–27.
- Woehrle, T., L. Yip, M. Manohar, Y. Sumi, Y. Yao, Y. Chen, and W.G. Junger. 2010. Hypertonic stress regulates T cell function via pannexin-1 hemichannels and P2X receptors. *J Leukoc Biol.* 88:1181–9.
- Yellen, G. 1998. The moving parts of voltage-gated ion channels. *Q Rev Biophys.* 31:239–95.

